

Dimensionally stable laminates under thermal loading and their applications

*Volodymyr Symonov**

Brno University of Technology, Institute of Aerospace Engineering, Aircraft design and test group,
616 69 Brno, Technická 2896/2, Czech Republic

Abstract. There exist many types of structures, which are required to have stable dimensions within a wide range of temperatures. The specific nature of composites allows finding special conditions when a laminate stacking sequence can provide zero thermal expansion coefficients in one or more directions. This allows the structure being designed to have the same dimensions in a wide range of temperatures. This work is aimed to find mathematical conditions, which guarantee in-plane zero CTE at least in one direction. As an application of thermally stable laminates a rotating disk is chosen. The mathematical model for such a disk is presented. Among investigated materials there was not found any of them, which can be used to layup a laminate with zero CTEs in two directions. However, all investigated materials can be used to layup many laminates with zero CTE in one or another direction. Moreover, it was discovered a laminate might have a zero CTE, if the lamina has zero or negative CTE at least in one direction. It was found the stresses, which appear in a laminated disk caused by centripetal forces, are insignificantly low in comparison to the thermal ones within the investigated ranges of angular velocity and temperature.

1 Introduction

Many structural applications of laminated FRP materials are connected with thermal loading, where special requirements are applied to the structure such as stability of its dimensions and/or shape within a certain range of temperatures. Mainly, these are the space applications, where the variation of geometry and/or shape of a special structure has strict limitations during its operation in order to keep their main characteristics. The examples of such structures can be space antennas, telescopes, instrumental platforms, etc. [1], [2], [3]. However, the ground applications are possible also. For example, the pressurized vessels and pipelines with a heated medium inside are discussed in [4].

Another possible future application could be a base-wheel and blades of a gas turbine engine, which are exposed to high temperatures and where the blade tip clearance represent a source of large loss in a turbine [5]. The less the gap the less loss. From the other hand, the thermal expansion of the wheel and blades is one of the reasons why it cannot be designed as small as possible for all engine modes.

The main reason for the laminated FRPs to be applied in above noted structures is an ability to control their properties via stacking sequence variation.

* Corresponding author: symonov@fme.vutbr.cz

The carbon-epoxy symmetrically balanced angle-ply laminates with almost null CTE in one direction firstly were found in [6], where the laminas' angles were approximately $\pm 42^\circ$. It was shown experimentally, the lamina CTEs are significantly changing within wide temperature range. Therefore, the found laminate has zero CTE only in narrow range close to room temperature.

Further T.Ishikawa et al. [7] proposed a technique for designing laminates, which have almost zero CTE in one direction in a wide temperature range. They used thermoelastic and in-plane stiffness invariants while finding the relation between the lamina thermal and mechanical properties and the laminate CTE in one direction. The technique is very good and simple for general case, when any type of laminate (orthotropic, anisotropic, etc.) is being looked for. However, the authors finally transit from the general case to the symmetrical balanced laminates like $[0^\circ, \pm\theta]_s$. In such a case it seems the relations and zero CTE laminates could be found in a more simple and evident way.

2 Zero CTE laminates

2.1 Formulation of the problem

The dimensionally stable laminate exposed to thermal loading (thermostable) is expressed by the next system of equations:

$$\begin{cases} \alpha_x = 0, \\ \alpha_y = 0, \end{cases} \quad (1)$$

where α_x and α_y – CTEs in the main directions of laminate's orthotropy (see Fig. 1).

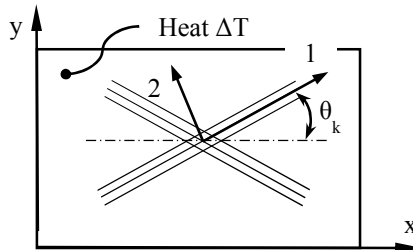


Fig. 1. Global laminate and local lamina coordinate systems.

It is required to develop a technique, which will help finding thermostable laminate(s) at least in one global direction within a narrow temperature range close to room temperature. The laminates being looked for are limited to the balanced symmetrical ones of $[0^\circ, 90^\circ, \pm\varphi]_{ns}$ class, where $\varphi \in (0^\circ, 90^\circ)$.

2.2 General thermo-mechanical equations

The stresses in k -th lamina caused by mechanical and thermal loading are given by [8]:

$$\begin{Bmatrix} \sigma_1 \\ \sigma_2 \\ \tau_1 \end{Bmatrix}_k = [Q]_k \left(\begin{Bmatrix} \varepsilon_1 \\ \varepsilon_2 \\ \gamma_1 \end{Bmatrix}_k - \begin{Bmatrix} \alpha_1 \\ \alpha_2 \\ 0 \end{Bmatrix}_k \Delta T \right), \quad (2)$$

where $[Q]_k$ – stiffness matrix of the k -th lamina; $\varepsilon_1, \varepsilon_2, \gamma_1$ – k -th lamina strains in local coordinate system; α_1, α_2 – CTEs of the k -th lamina in local coordinate system.

From other side, the laminate strains in laminate’s XOY coordinate system are:

$$\begin{pmatrix} \varepsilon_x \\ \varepsilon_y \\ \gamma_{xy} \end{pmatrix} = \begin{pmatrix} \alpha_x \\ \alpha_y \\ \alpha_{xy} \end{pmatrix} \Delta T. \tag{3}$$

Using the rotating matrix of the k -th lamina $[T]_k$, we can obtain lamina strains from (3):

$$\begin{pmatrix} \varepsilon_1 \\ \varepsilon_2 \\ \gamma_{12} \end{pmatrix}_k = ([T]_k^T)^{-1} \begin{pmatrix} \alpha_x \\ \alpha_y \\ \alpha_{xy} \end{pmatrix} \Delta T. \tag{4}$$

Finally, by substituting (4) to (2) and rotating stresses in k -th lamina from local coordinate system 12 to laminate’s XOY coordinate system we will obtain:

$$\begin{pmatrix} \sigma_x \\ \sigma_y \\ \tau_{xy} \end{pmatrix}_k = [T]_k^{-1} [Q]_k \left(([T]_k^T)^{-1} \begin{pmatrix} \alpha_x \\ \alpha_y \\ \alpha_{xy} \end{pmatrix}_k - \begin{pmatrix} \alpha_1 \\ \alpha_2 \\ 0 \end{pmatrix}_k \right) \Delta T. \tag{5}$$

Integration of (5) through the laminate thickness will give the next equation:

$$\begin{pmatrix} q_x \\ q_y \\ q_{xy} \end{pmatrix} = \sum_{k=1}^N \left(\int_{z_{k-1}}^{z_k} [\bar{Q}]_k dz \begin{pmatrix} \alpha_x \\ \alpha_y \\ \alpha_{xy} \end{pmatrix} \Delta T \right) - \sum_{k=1}^N \left(\int_{z_{k-1}}^{z_k} [\tilde{Q}]_k \begin{pmatrix} \alpha_1 \\ \alpha_2 \\ 0 \end{pmatrix}_k dz \Delta T \right), \tag{6}$$

where q_x, q_y, q_{xy} – the in-plane internal normal and shear forces, which appear in the laminate; N – the number of laminas in the laminate; z_k – the distance from the middle plane of the laminate to the lower surface of the k -th lamina; $[\bar{Q}]_k = [T]_k^{-1} [Q]_k ([T]_k^T)^{-1}$, $[\tilde{Q}]_k = [T]_k^{-1} [Q]_k$.

This equation can be written in the matrix form:

$$\{q\} = [A]\{\alpha^{xy}\}\Delta T - \{A_T\}, \tag{7}$$

where $A_{ij} = \sum_{k=1}^N (\bar{Q}_{ij})_k (z_k - z_{k-1})$, $A_{Ti} = \sum_{k=1}^N (\tilde{Q}_{ij})_k (z_k - z_{k-1})$.

If the structure is free of constrains and mechanical loading the internal forces are equal to zero, the solution of the equation (7) is the next:

$$\{\alpha^{xy}\} = [A]^{-1}\{A_T\}. \tag{8}$$

The equation (8) has the next unfolded view for orthotropic laminates:

$$\begin{pmatrix} \alpha_x \\ \alpha_y \\ \alpha_{xy} \end{pmatrix} = \begin{bmatrix} \frac{1}{HE_x} & -\frac{\mu_{yx}}{HE_y} & 0 \\ -\frac{\mu_{xy}}{HE_x} & \frac{1}{HE_y} & 0 \\ 0 & 0 & \frac{G_{xy}}{H} \end{bmatrix} \begin{pmatrix} A_{T1} \\ A_{T2} \\ 0 \end{pmatrix} \quad \text{or} \quad \begin{aligned} \alpha_x &= A_{T1} \frac{1}{HE_x} - A_{T2} \frac{\mu_{yx}}{HE_y}, \\ \alpha_y &= A_{T1} \frac{\mu_{xy}}{HE_x} + A_{T2} \frac{1}{HE_y}, \\ \alpha_{xy} &= 0, \end{aligned} \tag{9}$$

where H – is the total thickness of the laminate; $E_x, E_y, \mu_{xy}, \mu_{yx}, G_{xy}$ – are the elastic moduli, Poisson’s coefficients and the in-plane shear modulus of the laminate, respectively.

Finally, the thermostability conditions for orthotropic materials will have the next shape:

$$\begin{aligned}
 A_{T1} \frac{1}{HE_x} - A_{T2} \frac{\mu_{yx}}{HE_y} &= 0, \\
 A_{T1} \frac{\mu_{xy}}{HE_x} + A_{T2} \frac{1}{HE_y} &= 0,
 \end{aligned}
 \quad \text{or} \quad
 \begin{cases}
 A_{T1}A_{22} - A_{T2}A_{12} = 0, \\
 A_{T2}A_{11} - A_{T1}A_{12} = 0.
 \end{cases}
 \quad (10)$$

2.3 Themo stability conditions for $[0^\circ, 90^\circ, \pm\varphi]_{ns}$ laminates

The elements A_{ij} and A_{Ti} in a general case can be expanded as follows:

$$\begin{aligned}
 A_{11} &= \sum_{k=1}^N h_k [\bar{E}_{1k} \cos^4 \theta_k + 2\bar{E}_{1k} \mu_{21k} \sin^2 \theta_k \cos^2 \theta_k + \bar{E}_{2k} \sin^4 \theta_k + G_{12k} \sin^2 2\theta_k], \\
 A_{22} &= \sum_{k=1}^N h_k [\bar{E}_{1k} \sin^4 \theta_k + 2\bar{E}_{1k} \mu_{21k} \sin^2 \theta_k \cos^2 \theta_k + \bar{E}_{2k} \cos^4 \theta_k + G_{12k} \sin^2 2\theta_k], \\
 A_{12} &= \sum_{k=1}^N h_k \left[\frac{\bar{E}_{1k} + \bar{E}_{2k}}{4} \sin^2 2\theta_k + \bar{E}_{1k} \mu_{21k} (\sin^4 \theta_k + \cos^4 \theta_k) - G_{12k} \sin^2 2\theta_k \right],
 \end{aligned}
 \quad (11)$$

and

$$\begin{aligned}
 A_{T1} &= \sum_{k=1}^N h_k [\alpha_{1k} \bar{E}_{1k} (\cos^2 \theta_k + \mu_{21k} \sin^2 \theta_k) + \alpha_{2k} \bar{E}_{2k} (\sin^2 \theta_k + \mu_{12k} \cos^2 \theta_k)], \\
 A_{T2} &= \sum_{k=1}^N h_k [\alpha_{1k} \bar{E}_{1k} (\sin^2 \theta_k + \mu_{21k} \cos^2 \theta_k) + \alpha_{2k} \bar{E}_{2k} (\cos^2 \theta_k + \mu_{12k} \sin^2 \theta_k)].
 \end{aligned}
 \quad (12)$$

where h_k – the thickness of the k -th lamina; $\bar{E}_{ik} = \frac{E_{ik}}{1 - \mu_{12k} \mu_{21k}}, i = 1, 2$.

However, for $[0^\circ, 90^\circ, \pm\varphi]_{ns}$ laminates it can be significantly simplified.

Let's introduce the relative thicknesses of laminas group with the same orientation:

$$\psi_1 = \frac{h_{\Sigma 0}}{H}, \psi_2 = \frac{h_{\Sigma 90}}{H},
 \quad (13)$$

where $h_{\Sigma 0}, h_{\Sigma 90}$ – the total thicknesses of laminas group with orientation of 0° and 90° , respectively.

Thus, dividing the relationships (11) and (12) by the total thickness of the laminate and after some mathematical transformations we will obtain:

$$\begin{aligned}
 A_{T1} &= \psi_1 C_1 + \psi_2 C_2 + (1 - \psi_1 - \psi_2) [(C_1 - C_2) \cos^2 \varphi + C_2], \\
 A_{T2} &= \psi_1 C_2 + \psi_2 C_1 + (1 - \psi_1 - \psi_2) [(C_2 - C_1) \cos^2 \varphi + C_1], \\
 A_{11} &= \psi_1 \bar{E}_1 + \psi_2 \bar{E}_2 + (1 - \psi_1 - \psi_2) [\bar{E}_2 + 2D_2 \cos^2 \varphi - (D_1 + D_2) \cos^4 \varphi], \\
 A_{22} &= \psi_1 \bar{E}_2 + \psi_2 \bar{E}_1 + (1 - \psi_1 - \psi_2) [\bar{E}_1 + 2D_1 \cos^2 \varphi - (D_1 + D_2) \cos^4 \varphi], \\
 A_{12} &= (\psi_1 + \psi_2) \bar{E}_1 \mu_{21} + (1 - \psi_1 - \psi_2) [\bar{E}_1 \mu_{21} - (D_1 + D_2) (\cos^2 \varphi - \cos^4 \varphi)],
 \end{aligned}
 \quad (14)$$

where $C_1 = \alpha_1 \bar{E}_1 + \alpha_2 \bar{E}_2 \mu_{12}, C_2 = \alpha_2 \bar{E}_2 + \alpha_1 \bar{E}_2 \mu_{21}, D_1 = \bar{E}_1 \mu_{21} - \bar{E}_1 + 2G_{12}, D_2 = \bar{E}_1 \mu_{21} - \bar{E}_2 + 2G_{12}$.

After substitution (14) to (10) and mathematical transformations, the thermostability conditions (10) take the shape of two quadratic equations:

$$\begin{aligned} \beta \cos^2 2\varphi + 2(\beta_{11} + \beta) \cos 2\varphi + \beta + 2\beta_{11} + 4\beta_{12} &= 0, \\ \beta \cos^2 2\varphi + 2(\beta_{21} + \beta) \cos 2\varphi + \beta + 2\beta_{21} + 4\beta_{22} &= 0, \end{aligned} \tag{15}$$

where $\beta = (1 - \psi_1 - \psi_2)[A(C_2 + C_1) + (1 - \psi_1 - \psi_2)(C_2 - C_1)(\bar{E}_1 - \bar{E}_2)]$, $\beta_{i1} = (1 - \psi_1 - \psi_2)[(C_2 - C_1)(2\psi_i(\bar{E}_1 - \bar{E}_2) + \bar{E}_2 + \bar{E}_1\mu_{21}) + (C_2 + C_1)(2\bar{E}_1\mu_{21} + 4G_{12}) - 2\bar{E}_2C_1 - (\bar{E}_1 + \bar{E}_2)C_2]$, $\beta_{i2} = (\psi_i(C_2 - C_1) + C_1)(\psi_i(\bar{E}_1 - \bar{E}_2) + \bar{E}_2) - (\psi_i(C_1 - C_2) + C_2)\bar{E}_1\mu_{21}$.

These equations can be easily solved apart or as a system. Their roots give the angle φ in dependence to the mechanical and thermal properties of the lamina and to the relative thicknesses ψ_1 and ψ_2 . The first equation gives 3 parameters ψ_1, ψ_2 and φ at which the laminate has zero CTE in OX direction. The second equation gives these parameters for the case, when the laminate has zero CTE in OY direction.

2.4 Theoretical results

Many different materials were investigated for ability to build zero CTE laminates. There was not found any material, which can be used to layup a laminate with zero CTEs in two directions. However, many investigated materials can be used to layup many laminates with zero CTE in one or another direction. The Fig. 2 shows dependencies $\varphi = f(\psi_1, \psi_2)$ for zero CTE carbon-epoxy laminates, where the lamina properties are given in the Table 1.

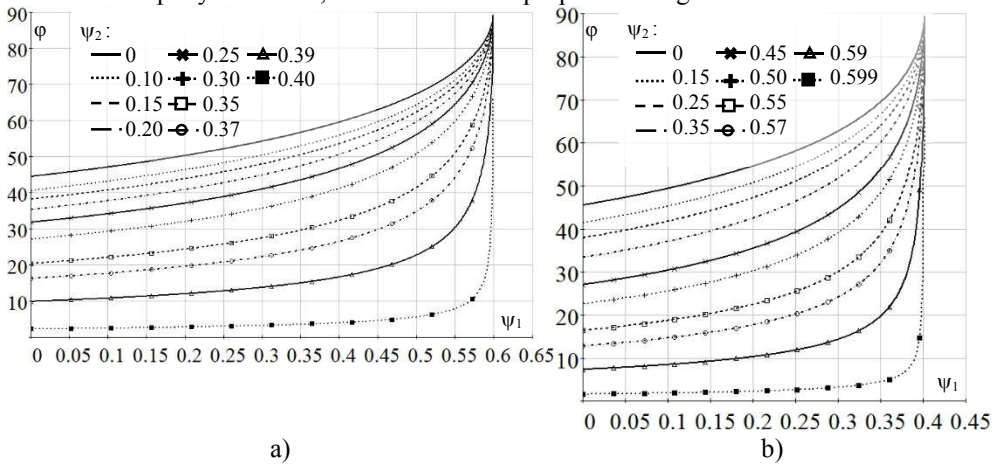


Fig. 2. Dependencies $\varphi = f(\psi_1, \psi_2)$ for laminates with: a) $\alpha_x = 0$, b) $\alpha_y = 0$.

Table 1. Properties of a unidirectional carbon-epoxy lamina.

P, kg/m ³	E ₁ , GPa	E ₂ , GPa	G ₁₂ , GPa	μ ₁₂	α ₁ , 1/K	α ₂ , 1/K	H, mm
1400	150	8	4	0.3	-2	40	0.12

3 Design of thermostable disks

3.1 Theoretical equations

Let us take an ideal case, when the shaft does not influence the disk and the stresses are not varying through the thickness of the disk. The main stresses are induced by centripetal forces and temperature loading. Let us assume the temperature field is constant within whole

disk, therefore the thermal stresses are constant everywhere also. The centripetal forces depend on the distance from the rotation axis only. Therefore, the stresses, which appear in the disk are the function of that distance also.

The small sector element of the disk with the dimensions of $dr \times d\theta$ (see Fig. 3a) is loaded on the edges and with the volumetric centripetal forces, which can be summarized to the resultant force:

$$dm = \frac{\rho}{g} H r^3 \omega^2 d\theta dr, \quad (16)$$

where $\frac{\rho}{g}$ – the specific weight of the material; H – the thickness of the disk.

The stresses' equilibrium in the disk can be expressed by the next differential equation:

$$r \frac{\partial \sigma_r}{\partial r} + \sigma_r - \sigma_\theta + \frac{\rho}{g} \omega^2 r^2 = 0. \quad (17)$$

The radial and circumferential stresses can be defined through the corresponding strains:

$$\begin{aligned} \sigma_r &= \bar{E}_r [\varepsilon_r + \varepsilon_\theta \mu_{\theta r} - \Delta T (\alpha_r + \alpha_\theta \mu_{\theta r})], \\ \sigma_\theta &= \bar{E}_\theta [\varepsilon_\theta + \varepsilon_r \mu_{r\theta} - \Delta T (\alpha_\theta + \alpha_r \mu_{r\theta})], \end{aligned} \quad (18)$$

where $\bar{E}_{r(\theta)} = \frac{E_{r(\theta)}}{1 - \mu_{r\theta} \mu_{\theta r}}$; E_r, E_θ – radial and circumferential elastic moduli of the laminate; α_r, α_θ – radial and circumferential CTEs of the laminate; $\mu_{\theta r}, \mu_{r\theta}$ – Poisson's coefficients of the laminate.

The radial and circumferential strains can be found easily:

$$\varepsilon_r = \frac{\partial u}{\partial r}, \varepsilon_\theta = \frac{u}{r}, \quad (19)$$

where u – is the radial displacements within the disk (see Fig. 3b).

After substituting (19) in to (18) and the results into (17) and mathematical transformations the next differential equation is obtained:

$$r \frac{\partial^2 u}{\partial r^2} + \frac{1}{r} \frac{\partial u}{\partial r} - k \frac{u}{r^2} = \frac{\Delta T}{r} [\alpha_r + \alpha_\theta \mu_{\theta r} - k(\alpha_\theta + \alpha_r \mu_{r\theta})] - \frac{\rho \omega^2 r}{\bar{E}_r g}, \quad (20)$$

where $k = \frac{\bar{E}_\theta}{\bar{E}_r}$.

The solution - the radial displacements in dependence to the radius is the next:

$$u(r) = \frac{r_2^2}{1 - k} \left[\frac{\Delta T}{r} (C_r - k C_\theta) - \frac{\rho \omega^2 r}{\bar{E}_r g} \right] + \bar{B} \left(\frac{r}{r_2} \right)^{\sqrt{k}} + \bar{D} \left(\frac{r}{r_2} \right)^{-\sqrt{k}}, \quad (21)$$

where r_2 – the outer radius of the disk; $C_r = \alpha_r + \alpha_\theta \mu_{\theta r}$; $C_\theta = \alpha_\theta + \alpha_r \mu_{r\theta}$; \bar{B}, \bar{D} – integration constants, which will be found later from the boundary conditions.

Finally, the radial and circumferential stresses can be found by substitution (21) into (19) and the result into (18):

$$\begin{aligned} \sigma_r &= \sigma_{rT} + \sigma_{r\omega}, \\ \sigma_\theta &= \sigma_{\theta T} + \sigma_{\theta\omega}, \end{aligned} \quad (22)$$

where $\sigma_{rT}, \sigma_{\theta T}$ - radial and circumferential thermal stresses, and $\sigma_{r\omega}, \sigma_{\theta\omega}$ - radial and circumferential stresses, caused by centripetal forces, which can be calculated as follows:

$$\begin{aligned} \sigma_{rT} &= \bar{E}_r \left\{ \Delta T \left[\frac{1}{1-k} \left(\frac{r_2}{r} \right)^2 (C_r - kC_\theta) (\mu_{\theta r} - 1) - C_r \right] + B_T (\mu_{\theta r} + \sqrt{k}) \frac{r^{-1+\sqrt{k}}}{r_2^{\sqrt{k}}} + \right. \\ &\quad \left. D_T (\mu_{\theta r} - \sqrt{k}) \sqrt{k} \frac{r^{-1-\sqrt{k}}}{r_2^{-\sqrt{k}}} \right\}, \\ \sigma_{\theta T} &= \bar{E}_\theta \left\{ \Delta T \left[\frac{1}{1-k} \left(\frac{r_2}{r} \right)^2 (C_r - kC_\theta) (1 - \mu_{r\theta}) - C_r \right] + B_T (1 + \sqrt{k} \mu_{r\theta}) \frac{r^{-1+\sqrt{k}}}{r_2^{\sqrt{k}}} + \right. \\ &\quad \left. D_T (1 - \sqrt{k} \mu_{r\theta}) \sqrt{k} \frac{r^{-1-\sqrt{k}}}{r_2^{-\sqrt{k}}} \right\}, \\ \sigma_{r\omega} &= \bar{E}_r \left\{ B_\omega (\mu_{\theta r} + \sqrt{k}) \frac{r^{-1+\sqrt{k}}}{r_2^{\sqrt{k}}} + D_\omega (\mu_{\theta r} - \sqrt{k}) \sqrt{k} \frac{r^{-1-\sqrt{k}}}{r_2^{-\sqrt{k}}} - C_\omega (\mu_{\theta r} + 1) \right\}, \\ \sigma_{\theta\omega} &= \bar{E}_\theta \left\{ B_\omega (1 + \sqrt{k} \mu_{r\theta}) \frac{r^{-1+\sqrt{k}}}{r_2^{\sqrt{k}}} + D_\omega (1 - \sqrt{k} \mu_{r\theta}) \sqrt{k} \frac{r^{-1-\sqrt{k}}}{r_2^{-\sqrt{k}}} - C_\omega (\mu_{\theta r} + 1) \right\}, \end{aligned} \quad (23)$$

where

$$\begin{aligned} B_T &= -\Delta T \frac{r_2 (1 - m^{-1-\sqrt{k}})}{(\mu_{\theta r} + \sqrt{k})(1 - m^{-2\sqrt{k}})} \left[\frac{1}{1-k} \frac{1 - m^{1-\sqrt{k}}}{1 - m^{-1-\sqrt{k}}} (C_r - kC_\theta) (\mu_{\theta r} - 1) - C_r \right], \\ D_T &= -\Delta T \frac{r_2 (m^{-1-\sqrt{k}} - m^{-2\sqrt{k}})}{(\mu_{\theta r} + \sqrt{k})(1 - m^{-2\sqrt{k}}) \sqrt{k}} \left[\frac{1}{1-k} \frac{1 - m^{1+\sqrt{k}}}{1 - m^{-1+\sqrt{k}}} (C_r - kC_\theta) (\mu_{\theta r} - 1) - C_r \right], \\ B_\omega &= \frac{r_2 (1 - m^{-1-\sqrt{k}}) C_\omega (\mu_{\theta r} + 1)}{(\mu_{\theta r} + \sqrt{k})(1 - m^{-2\sqrt{k}})}, \quad D_\omega = \frac{r_2 (m^{-1-\sqrt{k}} - m^{-2\sqrt{k}}) C_\omega (\mu_{\theta r} + 1)}{(\mu_{\theta r} + \sqrt{k})(1 - m^{-2\sqrt{k}})} \end{aligned}$$

are the integration constants; $C_\omega = \frac{\rho \omega^2 r_2^2}{g \bar{E}_r (1-k)}$; $m = \frac{r_2}{r_1}$; r_1 - the inner radius of the disk.

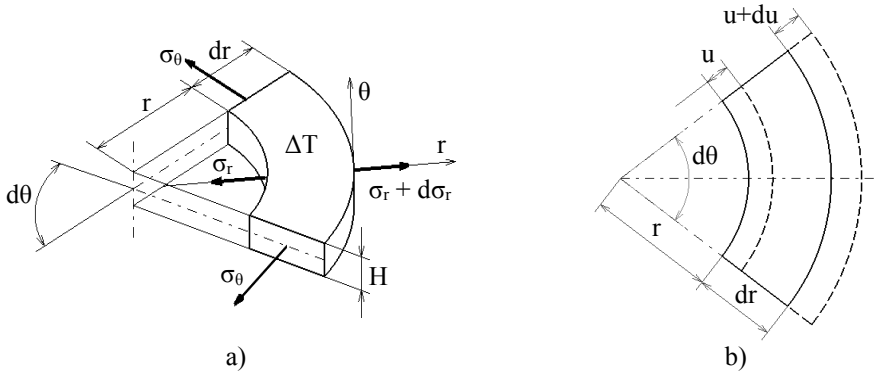


Fig. 3. Equilibrium of a disk element: a) stresses, which appear in the disk, b) displacements, which appear in the disk.

3.2 An example of stresses calculation

The parameters of the case being calculated are shown in the Table 2.

The lamina material has the properties, which are shown in the Table 1 above. Two stacking sequences $[0^\circ, 90^\circ]_{ns}$ are investigated. The first one has 60% of 0° layers and $\alpha_r = 0$. The second one has 40% of 0° layers and $\alpha_\theta = 0$.

Table 2. The parameters of the case.

r_1, m	r_2, m	ω, rps	$\Delta T, ^\circ C$
0.050	0.250	333.33	20

The distribution of radial and circumferential thermal, centripetal and total stresses along the disk radius are shown in the Fig. 4 - Fig. 5.

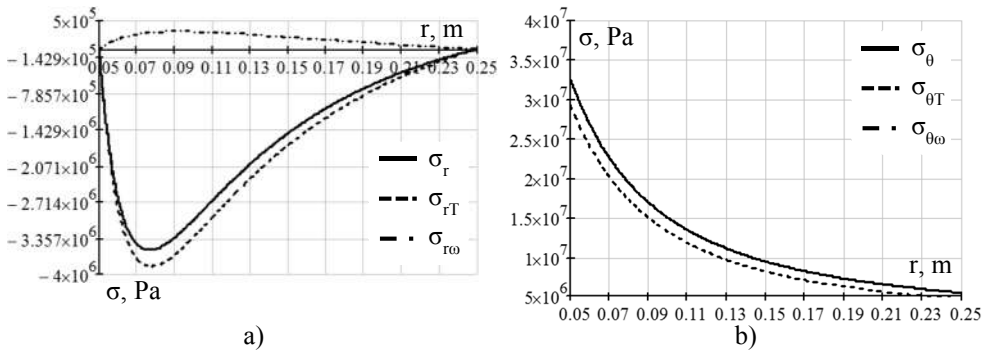


Fig. 4. Stresses for the first stacking sequence, $0^\circ - 60\%$, $\alpha_r = 0$: a) radial, b) circumferential.

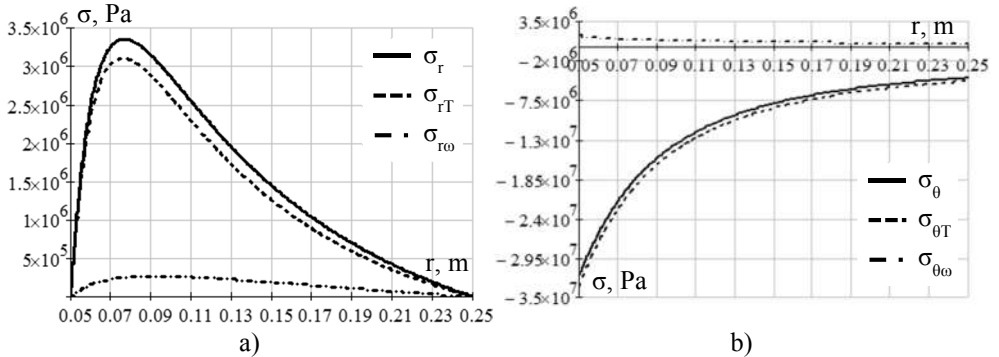


Fig. 5. Stresses for the second stacking sequence, $0^\circ - 40\%$, $\alpha_\theta = 0$: a) radial, b) circumferential.

The local lamina stresses in 1 and 2 directions of the local coordinate system for both sequences are shown below in the Fig. 6.

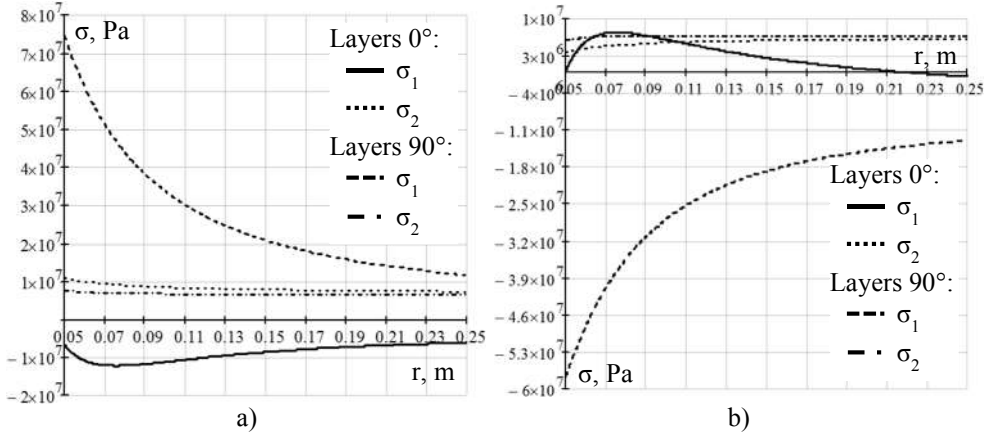


Fig. 6. Lamina stresses: a) for the first stacking sequence, 0° - 60%, $\alpha_r = 0$, b) for the second stacking sequence, 0° - 40%, $\alpha_\theta = 0$.

The radial and circumferential stresses induced by heat in relation to the total stresses for these two sequences, are shown below in the Fig. 7 and Fig. 8.

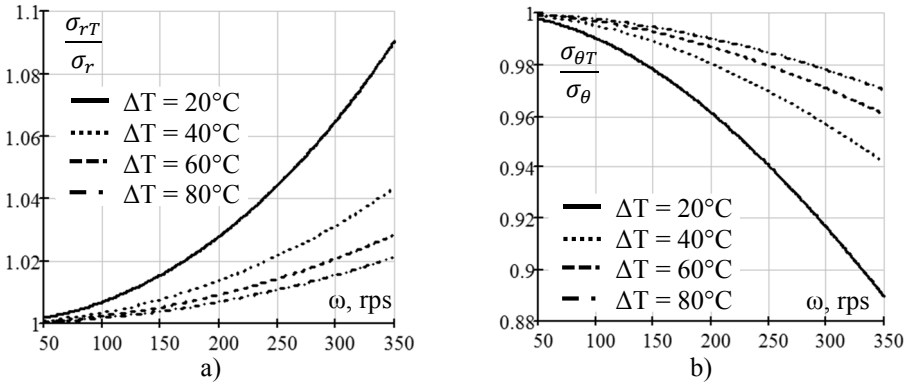


Fig. 7. Thermal stress in relation to the total stress for the first stacking sequence, 0° - 60%, $\alpha_r = 0$: a) in radial direction, b) in circumferential direction.

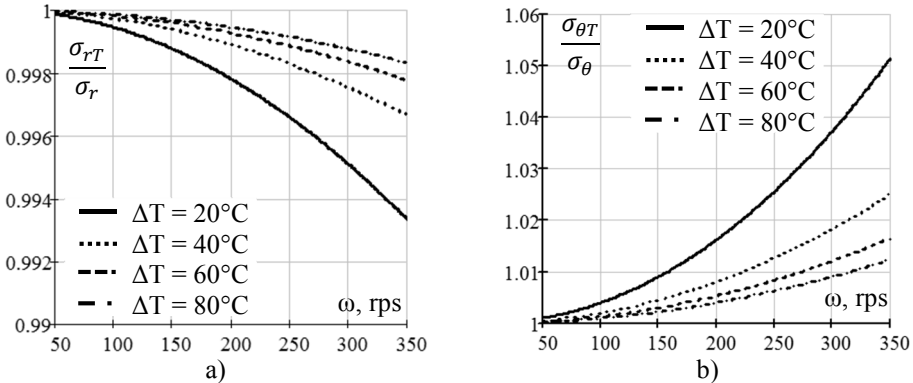


Fig. 8. Thermal stress in relation to the total stress for the second stacking sequence, 0° - 40%, $\alpha_\theta = 0$: a) in radial direction, b) in circumferential direction.

4 Conclusions

As the result of this work the in-plane thermostability condition is found for orthotropic laminates of $[0^\circ, 90^\circ, \pm\phi]_{ns}$ class. Many different materials were investigated for ability to build zero CTE laminates. There was not found any material, which can be used to layup a laminate with zero CTEs in two directions. However, many of the investigated materials can be used to layup many laminates with zero CTE in one or another direction. Moreover, it was discovered a laminate can have a zero CTE, if the lamina has zero or negative CTE at least in one direction.

A technique was developed for analytical calculation of stresses, which appear in a heated and rotating with a constant angular velocity disk made of laminate.

The stresses were investigated for a disk made of CFRP with two different $[0^\circ, 90^\circ]_{ns}$ stacking sequences. One of them had zero CTE in radial direction and another one - in circumferential direction. For the investigated ranges of angular velocity (166.67 - 333.33 rps) and temperature (40 - 100°C) it was found, the stresses caused by centripetal forces are insignificantly low in comparison to the thermal ones.

References

1. L. Datashvili, N. Nathrath, M. Lang, at el., New concepts and reflecting materials for space borne large deployable reflector antennas, Technical University of Munich, Germany (2014).
2. H. P. Gröbelbauer, M. Heer, Development of a Dimensionally Stable Lightweight Structure for the LISA Pathfinder Science Module (CEAS, Berlin, Germany, 2007).
3. G. Cherniavsky, A. A. Romanov, V. A. Tulmenkov, at el., Design and manufacturing of composite frame elements of optical-electronic unit of an automated space satellite (XX Intern. Sci. and Tech. Conf.: Struct. and Proc. for Manuf. Products from Nonmetal. Mater., Obninsk, Russia, 2013), [in Russian].
4. Y. Loskutov, A. Baev, L. Slavutskii, at el., Development of dimensionally stable structures of multilayer pipelines and cylindrical pressure vessels from carbon fiber reinforced plastic, East.-Eur. J. of Enterprise Technologies, **96**, 6/7, pp. 32-38 (2018).
5. C. Bringhenti, J. R. Barbosa, Effects of Turbine Tip Clearance on Gas Turbine Performance (ASME Turbo Expo, Berlin, Germany, 2008).
6. K. F. Rogers, L. N. Phillips, D. M. Kingston-Lee, at el., The thermal expansion of carbon fibre-reinforced plastics. Part 1: The influence of fibre type and orientation, *J. of Mater. Sci.*, **12**, pp. 718-734 (1977).
7. T. Ishikawa, H. FUKUNAGA, K.-I. ONO, Graphite-epoxy laminates with almost null coefficient of thermal expansion under a wide range of temperature, *J. of Mater. Sci.*, **24**, pp. 2011-2017 (1989).
8. R. F. Gibson, Principles of composite material mechanics, Detroit, Michigan, McGraw-Hill Inc., (1994).

Acknowledgement

This work was done with the financial support of the project TE02000032 “Advanced Aerostructures Research Centre” financed by the Technology Agency of the Czech Republic.